The influence of precursors on the induction period and transition-regime of dimethyl ether conversion to hydrocarbons over ZSM-5 catalysts

Toyin Omojola[a,b,*], Dmitry B. Lukyanov[a,*], Nikolay Cherkasov[b], Vladimir L. Zholobenko[c], André C. van Veen[b,*]

[a] Department of Chemical Engineering, University of Bath, Claverton Down, Bath, BA2 7AY, UK

[b] School of Engineering, University of Warwick, Library Road, Coventry, CV4 7AL, UK

[c] School of Physical and Chemical Sciences, Keele University, Staffordshire, ST5 5BG, UK

* Corresponding authors: toyin.omojola@bath.edu, d.b.lukyanonv@bath.ac.uk, andre.vanveen@warwick.ac.uk

Abstract

ZSM-5 catalysts were subjected to step response cycles of dimethyl ether (DME) at 300 °C in a temporal analysis of products (TAP) reactor. Propylene is the major olefin and displays an S-shaped profile. A 44-min induction period occurs before primary propylene formation and is ~~eliminated~~ reduced upon subsequent step response cycles. The S-shaped profile was interpreted according to induction, transition-regime and steady-state stages to investigate hydrocarbon formation from DME. The influence of precursors (carbon monoxide, hydrogen, dimethoxymethane, and 1,5-hexadiene) was studied using a novel consecutive step response methodology in the TAP reactor. Addition of dimethoxymethane, carbon monoxide, hydrogen and 1,5-hexadiene reduce the induction period of primary olefin formation. However, while dimethoxymethane, carbon monoxide and hydrogen accelerate the transition-regime towards hydrocarbon pool formation, 1,5-hexadiene attenuates it. Heavier hydrocarbons obtained from 1,5-hexadiene compete for active sites during secondary olefin formation from the aromatic dealkylation chemistry. A phenomenological evaluation of multiple parameters is presented.

Keywords

Methanol; Methanol-to-olefins; ZSM-5; Dimethyl Ether (DME); Temporal Analysis of Products (TAP) reactor; primary olefins; nucleation kinetics; dimethoxymethane (DMM); diene; transition-regime; induction period; hydrocarbon-pool; multi-parameter space evaluation

1. Introduction

Fuels and chemicals are increasingly produced from non-conventional carbon feedstock due to rising demand, a lack of secure resources and a need to reduce carbon footprint. Methanol can be obtained from renewable resources and converted to olefins (MTO) over zeolite catalysts. Although the MTO process has been commercialised[1], the mechanism underlying the formation of the first C-C bond and primary olefin(s) remains elusive.

The MTO process begins with methanol equilibration over fresh ZSM-5 zeolite catalysts[2,3]. Methanol and equilibration products i.e. dimethyl ether (DME) and water compete initially for active sites. The first C-C bond is then formed from these initial species as the zeolite is transformed from its fresh state *via* a transition-regime to its working state[4-7]. During its working state (i.e steady-state), a "hydrocarbon pool" mechanism (Figure 1) consisting of a dual cycle (an aromatic and an olefin cycle), regulates product distribution[8-10]. The pathway through which methanol and/or DME leads to the first C-C bond and primary olefin(s) during the induction period and the transition regime is currently debated[4,5,8-15].

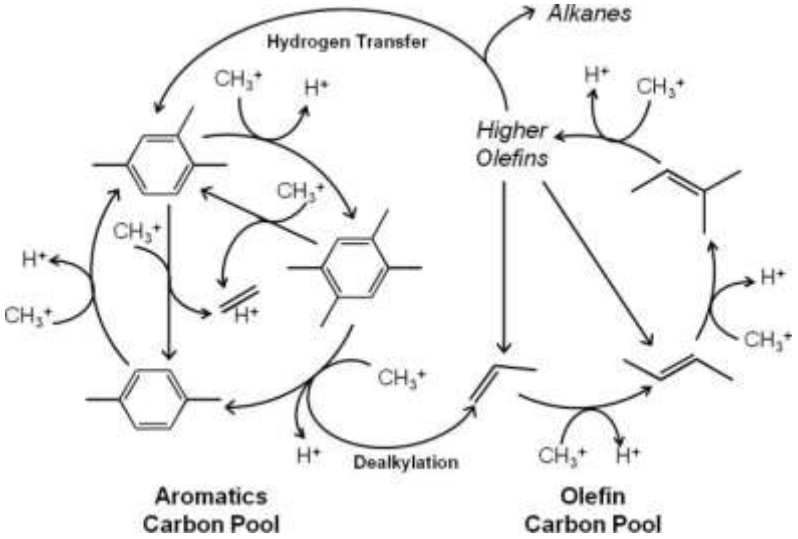

Figure 1: Dual-cycle during the conversion of methanol to hydrocarbons over zeolite catalysts. "Reprinted with permission from [16]. Copyright (2013) American Chemical Society."

Primary olefins could form directly[13,17-19] or indirectly[8-10,20] over ZSM-5 catalysts. Alkyl-substituted cyclopentenyl carbenium ions are a persistent intermediate closely associated with the indirect primary olefin formation pathway[21,22]. Cyclopentadiene, observed over zeotype catalysts[23], can be protonated into cyclopentenyl carbenium ions. The origin of the cyclopentenyl carbenium ions were initially proposed to be an artefact of impurities (ethanol, acetone) in the methanol feed[5]. Conversely, Novakova et al.[24], Liu et al.[15] and Chang et

Formatted: English (United Kingdom)
Field Code Changed
Formatted: Danish
Formatted: Danish
Field Code Changed
Field Code Changed

provided evidence for dimethoxymethane as a dominant intermediate in the direct pathway of primary olefin formation. Dimethoxymethane decomposes over ZSM-5 catalysts producing dimethyl ether, formaldehyde, methyl formate and methanol.[26] Methanol further decomposes on zeolites in the absence of Brønsted acid sites to carbon monoxide, hydrogen, formaldehyde and methane.[15] Carbon monoxide reacts with surface methoxy groups in a relatively low activation energy pathway (80 $kJmol^{-1}$) leading to primary olefins. Here, the relevant intermediates are acetyl groups, which dissociate into methyl acetate and acetic acid.[15,27,28] higher pressures (400 – 3,000 KPa), hydrogen is involved in hydrogen transfer pathways and intercepts the formation of deactivation-inducing polycyclic species, leading to increased catalyst stability.[29]

Haw and co-workers studied the induction period over zeolite and zeotype catalysts in a pulse-quench catalytic reactor using ^{13}C MAS NMR spectroscopy.[4-6,21,30,31] They observed that the active site during MTO conversion is a composite of well-defined organic species and one or more inorganic acid sites, which can activate methanol and hold methyl cation equivalents[30] and impurities such as ethanol and acetone control the induction period.[5,6,31] Qi et al.[32] studied the induction period under continuous flow at 245 – 280 °C and 1 bar. The transformation of the initial C-C bond to hydrocarbon pool species was observed to be rate-limiting in their proposed three-stage induction period of methanol conversion.[32] Co-feeding methanol with olefin precursors i.e. ethanol, propanol, hexan-1-ol and cyclohexanol[33] or aromatics i.e. benzene, toluene, p-xylene and naphthalene[32,34] reduces the induction period. A high zeolite acid site density increases the rate of formation of occluded species and their autocatalytic effect.[35] Lee et al.[36] showed that catalysts with larger crystals and smaller external surface area exhibit a longer induction period due to a smaller number of accessible channels. The response of the induction period to impurities and olefin and aromatic precursors is similar to a crystal nucleation process where seeding agents alter the rate of agglomeration.[37-39]

Temkin[40] distinguished two types of relaxation onto steady-state: (a) intrinsic relaxation, which is caused by the mechanism of the reaction itself, and (b) extrinsic relaxation, which is caused by modifications of the mechanism as a result of sub-surface chemistry. During the evolution from fresh to working state, intrinsic and extrinsic relaxation can be readily distinguished.[40,41] Kobayashi et al.[42-44] described various shapes and mechanisms underlying specie relaxation onto steady-state including: (1) the S-shaped profile where effluents form with an induction period, (2) overshoot profile where effluents initially exceed steady-state values and, (3) monotonic profiles where effluents begin to form immediately.

Higher temperatures are required to desorb DME in comparison to methanol from ZSM-5 catalysts[15,45,46] suggesting that DME is the key surface oxygenate at temperatures relevant to MTO. DME is constantly replenished from methanol, while being a constant supply

for the formation of aliphatics and aromatics during MTO conversion.[47] Transient microkinetic modelling studies[48] show that the transformation of the first C-C bond is rate-limiting in the induction period in accordance with previous studies by Qi et al.[32] The evolution of the hydrocarbon pool can be described not only by the induction-period chemistry, but also by the transition-regime and dual-cycle chemistry.[7,48] Here, we report the behaviour of precursors during the induction period and transition regime. Carbon monoxide, hydrogen, dimethoxymethane and 1,5-hexadiene were used to probe the evolution of the fresh catalyst to its working state when subject to a DME feed. A novel methodology was developed in a temporal analysis of products (TAP) reactor to understand precursor behaviour. Analysis was carried out using a logistic (sigmoidal) function for description of the induction period and the transition regime following crystal nucleation kinetics.

Dimethoxymethane, carbon monoxide and hydrogen were chosen following recent mechanistic insights obtained from the studies of Liu et al.[15] and Chowdhury et al.[14,49] on the influence of the products of methanol decomposition on the first C-C bond. On the other hand, 1,5-hexadiene was chosen as a model compound to simulate the effect of impurities, and consequently the indirect pathway of primary olefin formation. This is justified as dienes accept protons to first form reactive carbenium ions.[50,51] Cyclisation later occurs as the non-carbocationic unsaturated double bond attacks the postive cationic charge center closing the ring and resulting in alkylcyclopenta carbenium ions which form over ZSM-5 catalysts.[52,53] The study with dimethoxymethane gives the combined effect of DME, methyl formate, formaldehyde, methanol, carbon monoxide and hydrogen. The individualistic influence of carbon monoxide, and hydrogen was studied *via* co-feeding experiments.

2. Experimental

2.1. Materials

Fresh NH_4-ZSM-5 catalysts with Si/Al ratios of 11.5 and 25, referred to as ZSM-5 (11.5) and ZSM-5 (25) respectively, were purchased from Zeolyst International. The ammonium form of the zeolite was pressed, crushed, and sieved to obtain particle sizes in the range of 250 – 500 µm. Anhydrous DME (99.999%) and argon (99.999%) were purchased from CK Special Gases Ltd. Experiments were conducted in a transient reactor suited for the temporal analysis of products (TAP). The TAP reactor[54] consists of three chambers in series: (a) the reactor chamber, (b) the differential chamber and (c) detector chamber. The pressure at the exit of the reactor chamber is maintained at 10^{-5} Pa while the pressure at the end of the differential chamber is 10^{-6} Pa and QMS is 10^{-7} Pa. Further details on the TAP reactor can be found in section S1.

The response of the quadrupole mass spectrometer (QMS), placed in the detector chamber, was calibrated by passing continuous streams of various gases (methanol, DME, ethylene, propylene, etc.) in argon over an inert quartz bed with particle diameters between 355 – 500 µm. The low base pressure (10^{-7} Pa) in the detector chamber allows for high detection sensitivity necessary for quantitative analysis. The inert quartz bed used for calibration had the same length as the catalyst bed. The time required to reach steady state or to drop from steady state was fastest over the inert quartz bed (section S2). The normalised step function of DME over the quartz bed and over a ZSM-5 catalyst bed (Figure S1) was used to estimate a residence time of 45 s in the TAP reactor, according to the methodology described by Levenspiel.[55]

2.2. Characterisation

The ZSM-5 (25) catalyst has a crystallite size of 0.10 ± 0.02 µm, an apparent BET surface area[56] of 413 m^2 g^{-1}, 428 µmol g^{-1} of Brønsted acid sites (BAS), 35 µmol g^{-1} of Lewis acid sites (LAS) and a BAS/LAS ratio of 12.2. NH_4-ZSM-5 (25) loses 4.2 wt% of its initial mass under dry air heating in a thermogravimetric analyser (TGA) at 5 °C min^{-1} up until 600 °C.

ZSM-5 (11.5) catalyst is of roughly equal crystallite size as ZSM-5 (25). It has an apparent BET surface area[56] of 403 m^2 g^{-1},1120 µmol g^{-1} of BAS, 30 µmol g^{-1} of LAS and a BAS/LAS ratio of 38. NH_4-ZSM-5 (11.5) loses 10 wt% of its initial mass under dry air heating in the TGA at 5 °C min^{-1} up until 600 °C.

The XRD patterns of the two ZSM-5 samples and a reference ZSM-5 pattern are shown in Figure S2.1. All two samples are highly crystalline zeolites as with the standard MFI structure. Further characterisation details (XRD, SEM images, TGA) can be found in section S3.

2.3. Transient study

2.3.1. Methodology

10 mg of NH_4-ZSM-5 (25) catalyst was initially decomposed in the TAP reactor chamber by heating it at 10 °C min^{-1} up to 450 °C, holding for 30 min before bringing the sample to 300 °C. Background signal intensities were obtained. The catalyst was then subjected to a steady flow of argon at 10^{-8} $mols^{-1}$ in a first series of experiments. Afterwards, the flow was instantaneously switched to a feed of 5 vol% DME in argon (step-up) at a flow rate of 4.4×10^{-8} mol s^{-1}. At steady-state, the inlet DME feed was switched to a flow of argon (stopped-flow). A single step response cycle consists of three phases: step-up, steady-state and stopped-flow. Experiments involving multiple step response cycles were conducted and presented in a previous publication.[48]

In a second series of experiments, the influence of co-feeding carbon monoxide (0.33 vol%) and hydrogen (0.33 vol%) separately with the DME feed in a single step response cycle was studied over ZSM-5 (25) catalysts.

Lastly, precursors such as dimethoxymethane and 1,5-hexadiene were seeded separately in the TAP reactor before introduction of the DME feed using a novel consecutive step response methodology over ZSM-5 catalysts packed in a shallow bed in the TAP reactor. The consecutive step response experiments in the TAP reactor was implemented by conducting two step response cycles with different feeds: the first step-up cycle using the precursor (dimethoxymethane or 1,5-hexadiene) and the second step response cycle using 5 vol% DME at 300 °C over ZSM-5 (11.5) catalysts. As a baseline study for the consecutive step response experiments, 5 vol% DME over 10 mg of fresh ZSM-5 (11.5) catalysts was studied in a single step response cycle. To compare dimethoxymethane to 1,5-hexadiene, equimolar carbon input of the precursor was used. A step response of 2.5 vol% of 1,5-hexadiene was carried out on the reactor for 5, 15 and 90 min giving molar carbon input of 2.1, 6.53 and 39.2 µmol respectively followed by a step response of 5 vol% DME over the ZSM-5 (11.5) catalyst. Also, a step response of 5 vol% of dimethoxymethane was carried out for 5 min giving a molar carbon input of 1.9 µmol followed by a step response of 5 vol% DME over the ZSM-5 (11.5) catalyst. Thus, dimethoxymethane can be compared to 1,5-hexadiene after having seeded both precursors for 5 min each, while the effect of increasing molar carbon input can be observed with 1,5-hexadiene.

The influence of carbon monoxide and hydrogen were investigated *via* co-feeding while that of dimethoxymethane and 1,5-hexadiene were studied through seeding as the adsorption equilibrium of the former on bare non-modified zeolites is such that no appreciable coverage can be sustained under vacuum conditions. Redox sites are required to retain coverage. Conversely, dimethoxymethane and 1,5-hexadiene are susceptible to adsorption on acid sites following carbenium ion mechanism.

Flow rates of the inert feed similar to step response feed (*ca.* 10^{-8} $mols^{-1}$), inlet pressure below 1000 Pa[57] and reactor temperatures of 300 °C were used in all experiments. The active catalyst bed length was short (2 mm) compared to the overall bed length of 25 mm. The raw data (QMS ion currents) were corrected for background levels and fragmentation contributions for the different molecules and sensitivity factors (section S4).

Steady state DME conversion was calculated using equation 1:

$$X_{DME} = \frac{2\dot{n}_{DME,i} - (\dot{n}_{MeOH,e} + 2\dot{n}_{DME,e})}{2\dot{n}_{DME,i}} \quad (1)$$

where X_{DME} is the conversion of DME, $\dot{n}_{DME,i}$ is the molar feed flowrate of DME, $\dot{n}_{MeOH,e}$ is the effluent molar flowrate of methanol and $\dot{n}_{DME,e}$ is the effluent molar flowrate of DME. The reaction products observed under steady-state conditions showed no gaseous products

heavier than an m/z ratio of 56 (Figure S3). The induction period and growth rate of the transition-regime were analysed using the logistic (sigmoidal) function described in section 3.

2.4. Temperature programmed desorption (TPD)

TPD was carried out after every step response experiment by supplying argon at similar flow rates to the DME feed for 20 min to remove weakly adsorbed species from the ZSM-5 (25) catalyst and subjecting the zeolite to a linear temperature ramp at 15 °C min^{-1}. Analysis of the TPD profiles for estimation of maximum temperatures and activation energies of desorption were carried out using a microkinetic model described in our previous work[45].

After the third step response cycle at 300 °C, the ZSM-5 catalyst was heated up until 470 °C at 15 °C min^{-1} under argon flow. The response ($R = \frac{I_i - I_{bl}}{I_{Ar}}$) and normalised response ($R_N = \frac{R}{R_{Max}}$) were obtained. I_i is the ion current intensity at a specified m/z ratio, I_{bl} is the background intensity, I_{Ar} is the ion current intensity for argon and R_{max} is the maximum response value. The activation energies of the species desorbed were obtained for maximum temperatures of desorption of 400 and 460 °C.

3. Results

3.1. Step response

Figure 2, which has been reported before[48], shows the results of a step response experiment with 5 vol% DME at 300 °C. Propylene is the major olefin and exhibits an S-shaped profile. A 44-min induction period is observed before steady-state flow of propylene effluent in the first cycle. Methanol effluent displays a slight overshoot while water effluent displays a significant overshoot. DME effluent rises in two stages: first rapidly and then slowly onto its steady state value. In the initial transient phase, the DME and methanol effluent rise onto steady values, which are lower than the feed concentration. Water has a non-negligible induction period signifying that it is formed during the reaction and not desorbed from the reactor walls. The m/z ratio of 18 (Table S1) used to identify water has no contribution from any other hydrocarbons. Moreover, thermogravimetric analysis (TGA) of the NH_4-ZSM-5 (25) catalyst shows that it loses 4.2% of its initial mass at 600 °C. About 4% of its initial mass is lost at 450 °C indicating little loss of zeolite mass due to drying or decomposition of the zeolite above 450 °C. The prior calcination at 450 °C removes any residual water from the zeolite such that the water effluent observed in Figure 2 is generated from the reaction. The low selectivity to ethylene at low temperatures has been observed previously by Dewaele et al.[58]. Pérez-Uriarte et al.[59] also observed relatively high propylene selectivities at low temperatures with an increase in ethylene selectivity with temperature rise.

The second step response shows a different behaviour compared to the first step. After steady-state was achieved at 300 °C, the catalyst was purged by a flow of argon for 20 min starting at 80 min time on stream (TOS). A second step response cycle of 5 vol% DME was passed at 100 min TOS. The initial induction time of propylene effluent observed in the first step response cycle is removed. Propylene effluent maintains its S-shaped profile showing that no significant coke deposition had occurred. There is no overshoot in the water effluent on subsequent step response cycles. The DME effluent rises immediately in subsequent step response cycles in comparison to its slower pace in the first cycle.

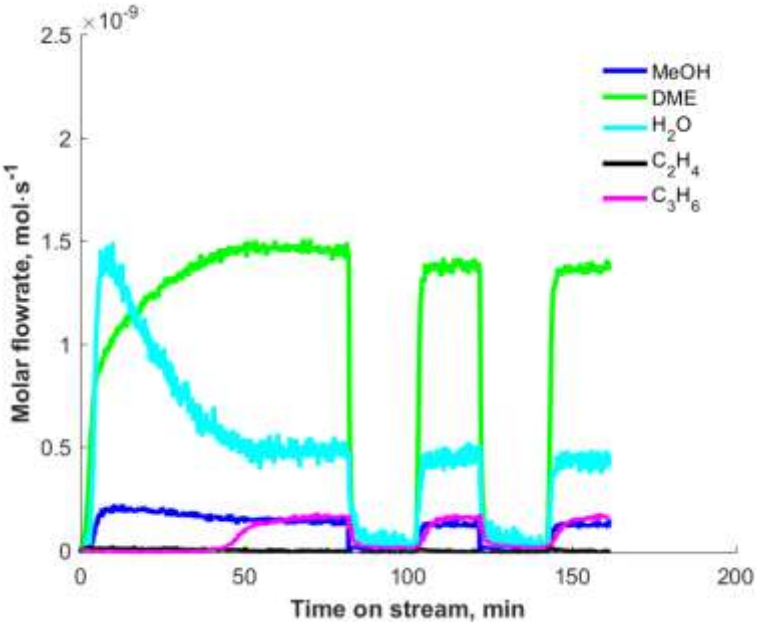

Figure 2: Step response of 5 vol% DME at 300 °C over 10 mg of ZSM-5 (25) catalysts. Total molar flow rate (5 vol% DME, balance Ar) = 4.4 × 10^{-8} mol s^{-1}. Steady state conversion is 34.8%. "Reprinted with permission from [48]. Copyright 2019. John Wiley & Sons."

3.2. Nature of occluded species using TPD of ZSM-5 (25)

The nature of the occluded species was studied by TPD of the ZSM-5 (25) catalyst after being subjected to multiple step response cycles at 300 °C. Figure S4 shows two groups of occluded species: (a) m/z ratio of 29, 31, 41 and 45 and (b) m/z ratio of 16, 18 and 91. These two groups can be distinguished based on their maximum temperatures (400 and 460 °C) and activation energies of desorption. Using m/z ratio of 41 as a proxy for the first group and m/z ratio of 91 for the second group, activation energies of desorption of 100 kJ mol^{-1} and 115 kJ mol^{-1} were obtained respectively. The low signal to noise ratio obtained in Figure S4 is evidence for weak signals of concentration profiles obtained during the step

response experiments. The first group (using m/z=41 as a proxy) and second group (using m/z=91 as a proxy) could be identified as fingerprints of the olefin and aromatic cycles respectively.

Although Figure S3 shows that no species heavier than m/z = 56 is present in the gas phase, the desorption of the working catalyst *via* TPD in Figure S4 shows that heavier products up until m/z = 91 are occluded in the spent catalyst. This behaviour has earlier been reported by Weisz and co-workers[60] who demonstrated product selectivity by showing that, of the many products that could be formed, only the molecules that can exit the pores based on their size appeared in the products.

Desorption profiles for dimethoxymethane and 1,5-hexadiene were obtained over ZSM-5 (25) catalysts. Dimethoxymethane shows reactive decomposition under vacuum at 15 °C min^{-1} (Figure S5a). 1,5-hexadiene undergoes molecular adsorption at low temperatures (< 200 °C) and dissociative adsorption at higher temperatures between 250 and 450 °C (Figure S5b). The desorption profiles of DMM and 1,5-hexadiene are compared to that obtained after a step response of DME over ZSM-5 (25) catalysts. The desorption profiles for DMM and 1,5-hexadiene show that they either exist in the pores of the catalyst or products of their dissociation are present in the pores of the catalyst at the step response temperatures. Further differentiation is obtained *via* the consecutive step response experiments described in section 3.4.

3.3. Co-feeding carbon monoxide or hydrogen with DME

Co-feeding of carbon monoxide or hydrogen with the DME feed was carried out over ZSM-5 (25) catalysts at 300 °C. Carbon monoxide and hydrogen are formed due to methanol decomposition on ZSM-5 catalysts. Consequently, co-feeding carbon monoxide or hydrogen should serves to subsequently increase their concentrations in the feed. Propylene effluent maintains its S-shape irrespective of the co-feed (Figure 3).

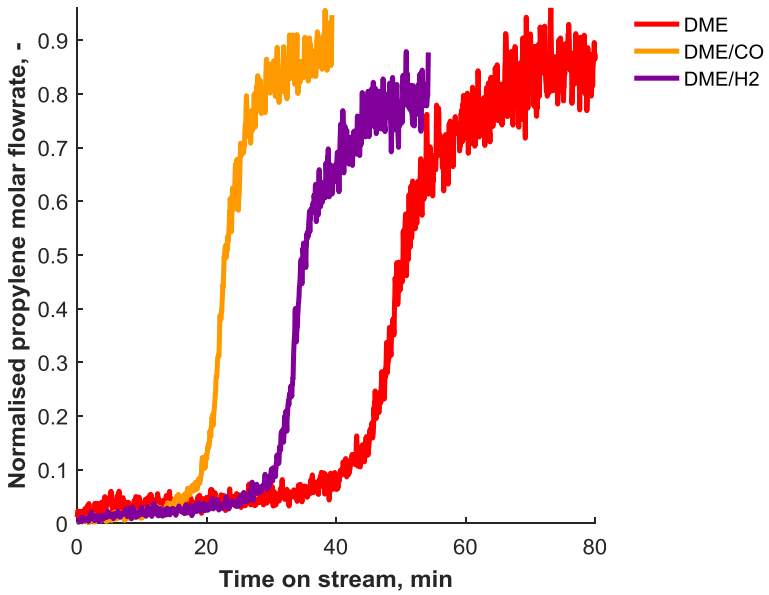

Figure 3: Effect of co-feeding (0.33 vol%) of carbon monoxide or hydrogen with 5 vol% DME on the induction period of propylene formation over ZSM-5 (25) catalysts at 300 °C. Raw data has been subject to noise filtering using a moving average of 3.

3.4. Consecutive step response experiments in the TAP reactor

Further experiments were carried out to distinguish the effect of 1,5-hexadiene and dimethoxymethane on a step response of DME in the TAP reactor. 5 vol% DME over 10 mg of fresh ZSM-5 (11.5) catalysts at 300 °C give an induction period and growth rate of hydrocarbon pool formation half and twice the induction period and growth rate of hydrocarbon pool formation over 10 mg of ZSM-5 (25) catalysts at 300 °C respectively. This suggests a relationship between the number of active sites, induction period and the rate at which the hydrocarbon pool is established at constant molar flowrate. After the consecutive step response experiments, temperature programmed desorption of occluded hydrocarbons in the ZSM-5 catalyst was carried out. Figure S6 gives the full consecutive-step response experiments of dimethoxymethane and 1,5-hexadiene over ZSM-5 (11.5) catalysts. In Figure S6a, no fragments of m/z = 41 are formed during DMM seeding, thus establishing the certainty of this assignment on introduction of DME in the second step response cycle. With 1,5-hexadiene in Figure S6b, certainty of this assignment arises from the observation that on removal of the precursor feed, the intensity of the fragment falls immediately and not slowly as would be the case for slow desorption. The m/z=41 fragment rises again on introduction of the DME feed in the second step response cycle. As can be observed, the rise rates of the

intensity of the m/z=41 fragment on introduction of the 1,5-hexadiene precursor and on introduction of DME are different further buttressing the fact that the former is due to the precursor and the latter is due to propylene formed from DME.

Several functions were used to model the S-shaped profile of propylene including the Avrami equation[61-63], Richards curve[64] and logistic (sigmoidal) function[65]. Of these, the S-shaped propylene profile was described by the logistic (sigmoidal) function. Accordingly, the S-shaped profile can be defined by: (i) an initial induction stage where no propylene is obtained, (ii) a subsequent transition (growth) stage in which propylene effluent flowrates increase rapidly, and (iii) a final steady-state stage, where propylene effluent flowrate reaches a plateau and the dual-cycle dominates. The S-shaped profile of propylene can be normalised, and the logistic function can be fitted to account for these various phases:

$$I(t) = \frac{I_{max}}{1 + e^{-k(t-t_m)}} \quad (2)$$

where $I(t)$ is the intensity at time t, I_{max} is the maximum intensity at the plateau phase of the S-shaped profile, t_m is the inflection time at which the growth rate reaches its maximum and k (min^{-1}) is the apparent rate constant for the growth phase (transition-regime). The induction time (min) is given in empirical parameters as:

$$t_{ind} = t_m - \frac{2}{k} \quad (3)$$

Analysis by a logistic (sigmoidal) function for description of the evolution of the hydrocarbon pool as the catalyst evolves from its fresh state to its working state allows for a relatively simple mathematical treatment, which prevents the problem of over-parameterisation when a full mechanistic model is rendered. A full mechanistic model encompassing the induction period, transition-regime and the dual cycle mechanism would require modelling of greater than 100 rate constants where steady-state chemistries are considered. These include: olefin methylation, oligomerisation and cracking, hydrogen transfer and cyclisation and aromatic methylation and dealkylation.[16] Even more, when such a detailed mechanism is simulated, it would be difficult to make collective predictions of the group of chemistries and their influence of precursors on the induction period, transition-regime or the dual-cycle directly in the S-shaped propylene profile. The logistic (sigmoidal) function avoids these difficulties mentioned above by modelling the propylene effluent. This is feasible by analogy as the induction period is influenced by impurities, olefin co-feeding or aromatic co-feeding, thus mirroring the behaviour of crystal nucleation kinetics. The impact of adsorbed intermediates is evinced in the logistic (sigmoidal) function as the S-shaped profile is due to a series of stable intermediates.[42-44]

~~3.7.~~3.6. Influence of precursors on the induction period and transition regime of conversion to hydrocarbons

An analysis of the S-shaped propylene profile with or without precursors was carried out using equations 2 and 3. Carbon monoxide and hydrogen reduce the induction period of propylene formation (table 1). The reduction of the induction period with a carbon monoxide co-feed is 1.5 times the reduction of the induction period with a hydrogen feed. A step response of 5 vol% DME over ZSM-5 (25) without any co-feed gives an induction time of 44 min and growth rate of the transition-regime of 0.34 min^{-1}. Carbon monoxide co-feed decreases the induction period of a DME only feed by 54% while hydrogen co-feed decreases the induction period by 34%. The growth rate of the transition-regime is increased with carbon monoxide (79%) and hydrogen (24%).

Table 1: Induction times and growth rate constants of the S-shaped propylene profile obtained from DME at 300 °C over ZSM-5 (25) catalysts

Co-feed	**t_{ind} (min)**	**k (min^{-1})**
None	43.5	0.34
CO (0.33 vol%)	19.9	0.61
Hydrogen (0.33 vol%)	28.6	0.42

Propylene effluent, on seeding with dimethoxymethane for 5 min, shows a similar profile shape as with the single step response cycle of DME (Figure 4).

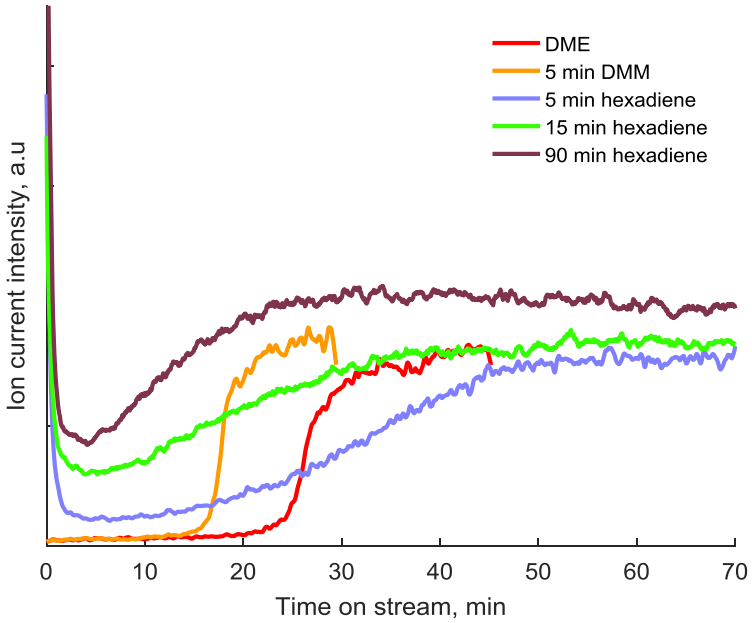

Figure 4: Comparison of induction times of propylene formation after its introduction in argon only (-); after introduction of a first step response cycle of 2.5 vol% 1,5-hexadiene for 5 (-), 15 (-) and 90 (-) min followed by a step response of 5 vol% DME in argon; after introduction of a first step response cycle of 5 vol% DMM for 5 min followed by a step response of 5 vol% DME in argon (-) over ZSM-5 (11.5) catalysts. Propylene is formed during the first step response of 2.5 vol% of 1,5-hexadiene. For brevity, only the effluents of the second step response cycle are shown (see Figure S6 for full consecutive step response methodology).

On addition of 1,5-hexadiene, the propylene effluent shows a different relaxation behaviour, although still exhibiting similar logistic characteristics to the single step response cycle of DME. The propylene effluent maintains an S-shaped profile irrespective of added precursors, as observed during the co-feeding experiments. A step response of DME over ZSM-5 (11.5) with no precursors give an induction time of 23 min and growth rate of the transition-regime of 0.63 min^{-1}. The induction time is reduced by 31 and 36% with roughly equimolar carbon input of dimethoxymethane and 1,5-hexadiene respectively (table 2).

Table 2: Induction times and growth rate constants of the S-shaped propylene profile obtained from DME at 300 °C over ZSM-5 (11.5) catalysts

Precursor	Seeding time of precursor (min)	Molar carbon input of precursor (µmol)	t_{ind} (min)	k (min^{-1})
None	-	-	23.2	0.63
DMM	5	1.90	15.9	1.02
1,5-hexadiene	5	2.10	14.8	0.15
1,5-hexadiene	15	6.53	4.28	0.18
1,5-hexadiene	90	39.2	1.07	0.26

However, while DMM increases the growth rate of the transition-regime of hydrocarbon pool formation by 62%, 1,5-hexadiene decreases the growth rate of the transition-regime of hydrocarbon pool formation by 76%. The growth rate increases further with increasing seeding time by 73% after 90 min in comparison to a seeding time of 5 min while the induction period drops.

4. Discussion

4.1. Step response study

During pulse measurements in the TAP reactor, a low detection limit and an unperturbed measurement of signal intensities due to the direct placement of the measuring probe in the detection chamber are implemented. Collisions between probe molecules and a complex solid, during Knudsen diffusion, may provide unique kinetic signatures contained in the motion of the molecules which are characteristic of the composition and structure of the catalyst surface.[66] This behaviour allows for kinetic investigations. The decrease in the contribution of re-adsorption phenomena and the removal of extra-particle mass transfer under vacuum conditions demonstrates its immense benefit.[45,67,68]

During step response experiments in the TAP reactor, low detection limits and an unperturbed measurement of signal intensities are still afforded. The influence of gaseous collisions between species and of collisions between the solid surface and gaseous species are relatively greater due to the flow conditions experienced during our step response experiments. Reduced pressure (<1000 Pa), however at these conditions, allows for reduced pressure gradients in the film surrounding the catalytic particle which, in the limits, are non-existent at the low pressures and ensuing densities. The dilute mixture also allows for negligible extra-particle heat transfer. Chansai et al.[69] presented a similar switching methodology as in our step response experiments albeit at much shorter time on stream and in a bench flow reactor. We note, however, that enhanced sensitivity in the TAP reactor used for step response experiments results from the transient techniques employed therein that

allow for decoupling of elementary steps in the induction period. Furthermore, the transfer function is virtually non-existent in the TAP reactor due to the free flight path at the end of the catalytic bed resulting in a negligible set-up contribution.

Initially, pulse studies of methanol and DME were carried out over ZSM-5 catalysts in the TAP reactor[45] with the aim of observing primary olefin formation. It became immediately clear that pulse studies were not ~~sufficient~~enough to unravel the complexity of the underlying mechanisms as methanol showed no outlet pulse over hydrocarbon-occluded ZSM-5 catalysts. The product desorption rates are much slower in comparison to formation rates such that the intensities observed during the pulse response is so small that it is observed in the noise of the sampling equipment. Nonetheless, we showed in ref.[45] that the temperature programmed desorption experiments used to probe desorption phenomena were carried out under intrinsic conditions following a methodology specified by Demmin and Gorte.[70] Similar phenomena has been observed on pulsing ammonia over Al-Sb-V-W oxide catalyst during propane ammoxidation in a TAP-2 reactor.[71] Consequently, our current methodology has involved the study of the preferential adsorption and desorption of methanol and DME over fresh and hydrocarbon occluded ZSM-5 catalysts of different Si/Al ratios.[45] Thereafter, a study of the evolution of hydrocarbons from DME using a novel methodology in the TAP reactor and identification of the rate-limiting steps in the induction period.[48] Here, we sought to understand the influence of various model precursors on the induction period and transition-regime before hydrocarbon pool formation.

A slow build-up of a steady pool of intermediates and their reaction to propylene occur during the first step response cycle (Figure 2) at 300 °C. The reaction of the DME feed with the occluded pool of intermediates is initiated during subsequent step response cycles. Heavier species are formed in the pores of the zeolite (Figure S4) compared to that observed in the gas phase (Figure S3). Therefore, the first cycle should involve intrinsic and extrinsic relaxation[40] describing the transformation due to the innate mechanism and pore chemistry respectively while the second and subsequent step response cycles should involve intrinsic relaxation only.

DME dissociates initially on acid sites and leads to the formation of surface methoxy groups and methanol. Methanol further dissociates leading to surface methoxy groups and water[13,45,72] or equilibrate leading to DME and water. Together, DME forms surface methoxy groups, methanol and water. Even in the absence of Brønsted acid sites, methanol decomposes to form carbon monoxide, formaldehyde, methane and hydrogen.[15] On further reaction, surface methoxy groups are converted into hydrocarbons and regenerate the active site.[18,19,73] Thus, the overshoot in water formation in Figure 2 can be described by two competing factors: (1) the generation of surface methoxy groups and methanol from DME and (2) the consumption of these adsorbed species towards hydrocarbon formation. These

competing factors could lead to an overshoot governed by the slow regeneration of active species (surface methoxy groups) or active sites on the catalyst surface.[42]

Reduction of the induction period in subsequent step cycles involves the co-operative nature of the incoming DME feed and the occluded hydrocarbons on the ZSM-5 catalyst.

4.2. Perspective on reaction mechanism

Initially, DME produces methanol, water, surface methoxy groups on its dissociation on Brønsted acid sites of the ZSM-5 catalyst. Recent studies show that surface methoxy groups[74] or formaldehyde[75] bound on extra framework aluminium sites could be critical C1 species from which the initial C-C bond is produced. With no co-feeding or precursor addition, DME converts directly to primary ethylene and/or propylene *via* the formation of adsorbed intermediates such as dimethoxymethane, dimethoxyethane and methyl propenyl ether[46,48,76] in the induction period. Dimethoxymethane decomposes on ZSM-5 catalysts to form DME (96.5%), methanol, formaldehyde and methyl formate.[26] Methanol further decomposes to form carbon monoxide, formaldehyde, methane and hydrogen, even in the absence of Brønsted acid sites.[15] Co-feeding with carbon monoxide or hydrogen increases their concentration during the propagation of the primary formation of ethylene and/or propylene. Carbonyl compounds such as methyl acetate and acetic acid have been observed on co-feeding methanol with carbon monoxide over zeolite catalysts.[14,15,49,77] Primary ethylene and/or propylene then forms higher olefin homologues through methylation with surface methoxy groups and cracking in the olefin cycle. Subsequent hydrogen transfer and cyclisation steps, and aromatic methylation and dealkylation lead to establishment of the dual cycle and production of secondary olefins. Thus, the total ethylene and propylene produced at steady-state can be conceived as a function of that produced primarily *via* dimethoxyethane and dimethoxymethane in the induction period and that obtained secondarily through the aromatic dealkylation chemistry in the aromatic cycle (Figure 5).

Alkylcyclopenta carbenium ions form methylbenzenes and primary ethylene and/or propylene indirectly in the induction period. 1,5-hexadiene is used as a model compound to initiate the formation of alkylcyclopenta carbenium ions[52,53] thus simulating the pathway previously observed with impurities by Haw and co-workers.[5] The formation of coke species could also result from these precursors (alkylcyclopenta carbenium ions and methylbenzenes). However, as observed in our TAP studies, the ZSM-5 catalysts were stable through multiple step response (Figure 2). Primary olefins (ethylene and/or propylene) formed from the 1,5-hexadiene *via* alkylcyclopenta carbenium ions in the induction period could further be methylated by surface methoxy groups and subsequent olefin homologues crack through the olefin cycle. Thereafter, hydrogen transfer and cyclisation steps, as well as further aromatic methylation and dealkylation steps complete the dual cycle. Thus, the total ethylene and

propylene produced at steady-state can be conceived as a function of that produced primarily by alkyl cyclopenta carbenium ions and methylbenzenes in the induction period and that produced secondarily by the dual cycle (Figure 5).

The difference between both pathways (dimethoxymethane, carbon monoxide and hydrogen; 1,5-hexadiene) is that heavier hydrocarbons are formed before the formation of primary olefins with 1,5-hexadiene while the heavy aromatics are formed after the formation of primary olefins with dimethoxymethane, carbon monoxide and hydrogen (Figure 5).

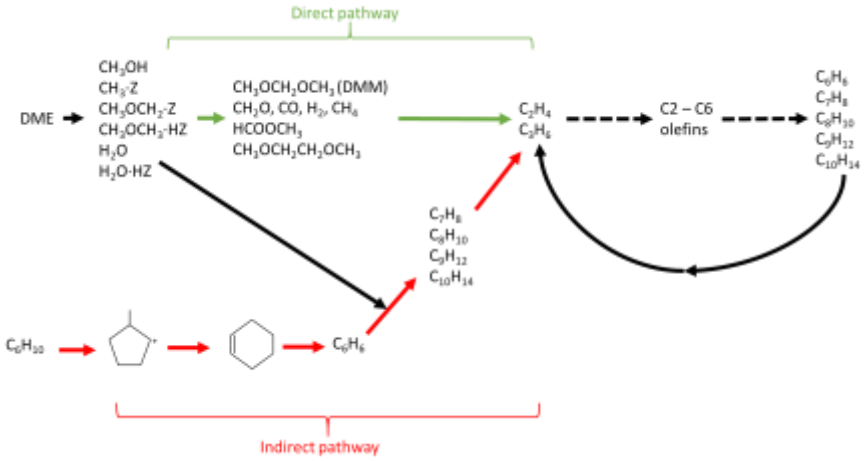

Figure 5: Proposed scheme of competing direct (—) and indirect (—) pathways to primary olefin formation from DME over ZSM-5 catalysts. Transition (growth) chemistry is given by (**- - -**).

As shown in tables 1 and 2, increasing the concentrations of carbon monoxide, hydrogen and dimethoxymethane all reduce the induction period. Carbon monoxide is 1.5 times as effective as hydrogen in reducing the induction period. The reduction of the induction period by carbon monoxide and dimethoxymethane following a spike in their concentrations may allow for faster rates of formation of intermediates (methyl acetate, surface acetates [14,15,49]) and could lead to faster rates of hydrocarbon pool formation. The reasons for reduction of the induction period and increase in the rate of hydrocarbon pool formation with hydrogen addition are less evident. Nonetheless, according to the framework developed in Figure 5, it is proposed that hydrogen reduces the induction period through increases in its concentration during primary olefin formation. Hydrogen also increases the growth rate of hydrocarbon pool formation due to its involvement in hydrogen transfer reactions in the formation of secondary olefins [16].

The formation of alkylcyclopenta carbenium ions through 1,5-hexadiene reduces the induction period by the same amount as dimethoxymethane. A high concentration of alkyl cyclopenta carbenium ions reduces the induction period as shown when the introduction of

these precursors is increased from 5 min to 90 min. The mechanism governing the influence of 1,5-hexadiene on the induction period is evident following the work of Haw and co-workers.[30] Here, simulating impurities by increasing the concentrations of 1,5-hexadiene could reduce the induction period by faster rates of methylbenzene formation and subsequent propagation to primary olefins as depicted in Figure 5. However, seeding with 1,5-hexadiene reduces the growth rate of the transition-regime of hydrocarbon pool formation (table 2). Two factors could be responsible: (1) the formation of coke species which deactivate the catalyst and/or (2) formation of heavy hydrocarbons/aromatics[52] from alkylcyclopenta carbenium ions which compete for active sites. The potential for coke deposition is reduced at low pressure and the deactivation is unlikely in our experiments as evinced by similar DME reactivity during the sequence of the step response experiments presented in this work. Hence, the data suggests that seeding with 1,5-hexadiene reduces the rate of hydrocarbon pool establishment in the transition regime is likely due to increased competition for active sites by heavier hydrocarbons formed *a priori*. The heavy hydrocarbons are formed during seeding with 1,5-hexadiene before initial ethylene and/or propylene formation. Subsequently, these heavy hydrocarbons compete for active sites with chemistries that establish the dual-cycle during the transition-regime.

Extensive spectroscopic (transmission FTIR) experiments (section S9) compared hydrocarbon-occluded ZSM-5 catalysts to experiments where 1,5-hexadiene, and dimethoxymethane were activated on fresh ZSM-5 catalysts to further understand the behaviour of these precursors. The results showed that no differentiation can be made based on FTIR alone.

Further evidence is provided from the TPD profiles of dimethoxymethane (Figure S5a) and 1,5-hexadiene (Fig S5b). Products of decomposition of 1,5-hexadiene only exit the zeolite pore system at temperatures between 250 and 450 °C. At a step response temperature of 300 °C, these products of decomposition of 1,5-hexadiene are still occluded in the pores. It can be conceived that these decomposition/reaction products compete for active sites at step response temperatures. However, the TPD profiles of dimethoxymethane shows that major products of decomposition exit the zeolite pore structure before step response temperature suggesting less competition for active sites. Evidently, dimethoxymethane still leads to propylene formation (Figure S5a).

We showed previously that the transformation of the first C-C bond is rate-limiting in the conversion of DME to primary olefins.[48] This was observed by Qi et al.[32] for MTO conversion. Herein, we show further that increasing the concentration of precursors i.e. carbon monoxide, hydrogen, dimethoxyethane and 1,5-hexadiene reduces the induction period and thus alleviates the bottleneck (rate-limiting) process in the conversion of DME to primary olefins. However, formation of heavier hydrocarbons from 1,5-hexadiene compete with the

transformation of these primary olefins thus reducing the rate of establishment of the dual cycle during the conversion of dimethyl ether to hydrocarbons.

5. Conclusions

The behaviour of precursors (carbon monoxide, hydrogen, dimethoxymethane, 1,5-hexadiene) during the induction period and transition-regime of the conversion of dimethyl ether to olefins over ZSM-5 catalysts has been studied in a temporal analysis of products reactor at 300 °C. Propylene is the major olefin and a 44-min induction period is observed in its formation during the first step response cycle, which is reducedeliminated on the second and subsequent step response cycles.

Propylene displays an S-shaped profile similar to the logistic (sigmoidal) behaviour as observed with a crystal nucleation mechanism. Propylene is primarily formed through a series of slowly generated adsorbed intermediates in the induction period and supplemented with the secondary formation *via* the aromatic dealkylation chemistry once the dual-cycle is established. Seeding with carbon monoxide, hydrogen and dimethoxymethane increases their concentrations in the induction period on introduction of the DME feed. Conversely, on seeding with 1,5-hexadiene, the primary olefins are generated indirectly by the aromatic dealkylation chemistry and secondary olefin formation occurs *via* after the establishment of the dual cycle.

The induction period is decreased on addition of dimethoxymethane, carbon monoxide and hydrogen. The growth rate of the transition-regime of hydrocarbon pool formation is also increased by addition of these precursors. Conversely, 1,5-hexadiene reduces both the induction period of propylene formation and the growth rate of the transition-regime of hydrocarbon pool formation due to competition with heavier intermediates formed *a priori* for active sites.

6. Supplementary Information

Relevant details about the TAP reactor, blanck experiments, characterization of ZSM-5 catalysts by XRD, SEM and TGA, analysis procedures, spectrum of species at steady-state, TPD of working catalyst, TPD of dimethoxymethane and 1,5-hexadiene, consecutive step response methodology and transmission FTIR experiments.

7. Author information

Corresponding authors: toyin.omojola@bath.edu, d.b.lukyanov@bath.ac.uk, andre.vanveen@warwick.ac.uk

ORCID

Toyin Omojola: 0000-0001-9376-6977

8. Notes

The authors declare no conflict of interest.

9. Acknowledgements

Financial support from the Petroleum Technology Development Fund of Nigeria (PTDF/ED/PHD/OO/766/15) and from the European Commission in the scope of the 7th Framework program BIOGO project (grant number: 604296) https://www.biogo.eu/ is acknowledged.

10. References

(1) Tian, P.; Wei, Y.; Ye, M.; Liu, Z. Methanol to olefins (MTO): From fundamentals to commercialization. *ACS Catalysis.* **2015**, *5*, 1922-1938.

(2) Svelle, S.; Kolboe, S.; Swang, O.; Olsbye, U. Methylation of Alkenes and Methylbenzenes by Dimethyl Ether or Methanol on Acidic Zeolites. *The Journal of Physical Chemistry B.* **2005**, *109*, 12874-12878.

(3) Svelle, S.; Visur, M.; Olsbye, U.; Saepurahman; Bjørgen, M. Mechanistic aspects of the zeolite catalyzed methylation of alkenes and aromatics with methanol: A review. *Top. Catal.* **2011**, *54*, 897-906.

(4) Goguen, P. W.; Xu, T.; Barich, D. H.; Skloss, T. W.; Song, W.; Wang, Z.; Nicholas, J. B.; Haw, J. F. Pulse-quench catalytic reactor studies reveal a carbon-pool mechanism in methanol-to-gasoline chemistry on zeolite HZSM-5. *J. Am. Chem. Soc.* **1998**, *120*, 2650-2651.

(5) Song, W.; Marcus, D. M.; Fu, H.; Ehresmann, J. O.; Haw, J. F. An oft-studied reaction that may never have been: Direct catalytic conversion of methanol or dimethyl ether to hydrocarbons on the solid acids HZSM-5 or HSAPO-34. *J. Am. Chem. Soc.* **2002**, *124*, 3844-3845.

(6) Haw, J. F.; Song, W.; Marcus, D. M.; Nicholas, J. B. The Mechanism of Methanol to Hydrocarbon Catalysis. *Acc. Chem. Res.* **2003**, *36*, 317-326.

(7) Wang, S.; Chen, Y.; Qin, Z.; Zhao, T.-S.; Fan, S.; Dong, M.; Li, J.; Fan, W.; Wang, J. Origin and evolution of the initial hydrocarbon pool intermediates in the transition period for the conversion of methanol to olefins over H-ZSM-5 zeolite. *J. Catal.* **2019**, *369*, 382-395.

(8) Dahl, I. M.; Kolboe, S. On the reaction mechanism for propene formation in the MTO reaction over SAPO-34. *Catal. Lett.* **1993**, *20*, 329-336.

(9) Dahl, I. M.; Kolboe, S. On the Reaction Mechanism for Hydrocarbon Formation from Methanol over SAPO-34. I. Isotopic Labeling Studies of the Co-Reaction of Ethene and Methanol. *J. Catal.* **1994**, *149*, 458-464.

(10) Dahl, I. M.; Kolboe, S. On the reaction mechanism for hydrocarbon formation from methanol over SAPO-34: 2. Isotopic labeling studies of the Co-reaction of propene and methanol. *J. Catal.* **1996**, *161*, 304-309.

(11) Lesthaeghe, D.; Van Speybroeck, V.; Marin, G. B.; Waroquier, M. Understanding the failure of direct C-C coupling in the zeolite-catalyzed methanol-to-olefin process. *Angewandte Chemie - International Edition.* **2006**, *45*, 1714-1719.

(12) Lesthaeghe, D.; Van Speybroeck, V.; Marin, G. B.; Waroquier, M. The rise and fall of direct mechanisms in methanol-to-olefin catalysis: An overview of theoretical contributions. *Ind. Eng. Chem. Res.* **2007**, *46*, 8832-8838.

(13) Yamazaki, H.; Shima, H.; Imai, H.; Yokoi, T.; Tatsumi, T.; Kondo, J. N. Direct production of propene from methoxy species and dimethyl ether over H-ZSM-5. *Journal of Physical Chemistry C.* **2012**, *116*, 24091-24097.

(14) Chowdhury, A. D.; Houben, K.; Whiting, G. T.; Mokhtar, M.; Asiri, A. M.; Al-Thabaiti, S. A.; Basahel, S. N.; Baldus, M.; Weckhuysen, B. M. Initial Carbon–Carbon Bond Formation during the Early Stages of the Methanol-to-Olefin Process Proven by Zeolite-Trapped Acetate and Methyl Acetate. *Angewandte Chemie - International Edition.* **2016**, *55*, 15840-15845.

(15) Liu, Y.; Müller, S.; Berger, D.; Jelic, J.; Reuter, K.; Tonigold, M.; Sanchez-Sanchez, M.; Lercher, J. A. Formation Mechanism of the First Carbon-Carbon Bond and the First Olefin in the Methanol Conversion into Hydrocarbons. *Angewandte Chemie - International Edition.* **2016**, *55*, 5723-5726.

(16) Ilias, S.; Bhan, A. Mechanism of the catalytic conversion of methanol to hydrocarbons. *ACS Catalysis.* **2013**, *3*, 18-31.

(17) Yamazaki, H.; Shima, H.; Imai, H.; Yokoi, T.; Tatsumi, T.; Kondo, J. N. Evidence for a "carbene-like" intermediate during the reaction of methoxy species with light alkenes on H-ZSM-5. *Angewandte Chemie - International Edition.* **2011**, *50*, 1853-1856.

(18) Wang, W.; Buchholz, A.; Seiler, M.; Hunger, M. Evidence for an Initiation of the Methanol-to-Olefin Process by Reactive Surface Methoxy Groups on Acidic Zeolite Catalysts. *J. Am. Chem. Soc.* **2003**, *125*, 15260-15267.

(19) Wang, W.; Seiler, M.; Hunger, M. Role of surface methoxy species in the conversion of methanol to dimethyl ether on acidic zeolites investigated by in situ stopped-flow MAS NMR spectroscopy. *J. Phys. Chem. B.* **2001**, *105*, 12553-12558.

(20) Svelle, S.; Joensen, F.; Nerlov, J.; Olsbye, U.; Lillerud, K. P.; Kolboe, S.; Bjørgen, M. Conversion of methanol into hydrocarbons over zeolite H-ZSM-5: Ethene formation is mechanistically separated from the formation of higher alkenes. *J. Am. Chem. Soc.* **2006**, *128*, 14770-14771.

(21) Haw, J. F.; Nicholas, J. B.; Song, W.; Deng, F.; Wang, Z.; Xu, T.; Heneghan, C. S. Roles for cyclopentenyl cations in the synthesis of hydrocarbons from methanol on zeolite catalyst HZSM-5. *J. Am. Chem. Soc.* **2000**, *122*, 4763-4775.

(22) Wulfers, M. J.; Jentoft, F. C. The role of cyclopentadienium ions in methanol-to-hydrocarbons chemistry. *ACS Catalysis.* **2014**, *4*, 3521-3532.

(23) Dai, W.; Wang, C.; Dyballa, M.; Wu, G.; Guan, N.; Li, L.; Xie, Z.; Hunger, M. Understanding the Early Stages of the Methanol-to-Olefin Conversion on H-SAPO-34. *ACS Catalysis.* **2015**, *5*, 317-326.

(24) Nováková, J.; Kubelková, L.; Dolejšek, Z. Primary reaction steps in the methanol-to-olefin transformation on zeolites. *J. Catal.* **1987**, *108*, 208-213.

(25) Chang, C. D.; Silvestri, A. J. The conversion of methanol and other O-compounds to hydrocarbons over zeolite catalysts. *J. Catal.* **1977**, *47*, 249-259.

(26) Fu, Y.; Zhu, H.; Shen, J. Thermal decomposition of dimethoxymethane and dimethyl carbonate catalyzed by solid acids and bases. *Thermochim. Acta.* **2005**, *434*, 88-92.

(27) Plessow, P. N.; Studt, F. Unraveling the Mechanism of the Initiation Reaction of the Methanol to Olefins Process Using ab Initio and DFT Calculations. *ACS Catalysis.* **2017**, *7*, 7987-7994.

(28) Plessow, P. N.; Studt, F. Theoretical Insights into the Effect of the Framework on the Initiation Mechanism of the MTO Process. *Catal. Lett.* **2018**, *148*, 1246-1253.

(29) Arora, S. S.; Nieskens, D. L. S.; Malek, A.; Bhan, A. Lifetime improvement in methanol-to-olefins catalysis over chabazite materials by high-pressure H2 co-feeds. *Nature Catalysis.* **2018**, *1*, 666-672.

(30) Song, W.; Haw, J. F.; Nicholas, J. B.; Heneghan, C. S. Methylbenzenes are the organic reaction centers for methanol-to-olefin catalysis on HSAPO-34. *J. Am. Chem. Soc.* **2000**, *122*, 10726-10727.
(31) Song, W.; Nicholas, J. B.; Haw, J. F. A persistent carbenium ion on the methanol-to-olefin catalyst HSAPO-34: Acetone shows the way. *J. Phys. Chem. B.* **2001**, *105*, 4317-4323.
(32) Qi, L.; Wei, Y.; Xu, L.; Liu, Z. Reaction Behaviors and Kinetics during Induction Period of Methanol Conversion on HZSM-5 Zeolite. *ACS Catalysis.* **2015**, *5*, 3973-3982.
(33) Langner, B. E. Reactions of methanol on zeolites with different pore structures. *Applied Catalysis.* **1982**, *2*, 289-302.
(34) Qi, L.; Li, J.; Wei, Y.; Xu, L.; Liu, Z. Role of naphthalene during the induction period of methanol conversion on HZSM-5 zeolite. *Catalysis Science and Technology.* **2016**, *6*, 3737-3744.
(35) Qi, L.; Li, J.; Wei, Y.; He, Y.; Xu, L.; Liu, Z. Influence of acid site density on the three-staged MTH induction reaction over HZSM-5 zeolite. *RSC Advances.* **2016**, *6*, 52284-52291.
(36) Lee, K. Y.; Chae, H. J.; Jeong, S. Y.; Seo, G. Effect of crystallite size of SAPO-34 catalysts on their induction period and deactivation in methanol-to-olefin reactions. *Applied Catalysis A: General.* **2009**, *369*, 60-66.
(37) Nielsen, L.; Khurana, R.; Coats, A.; Frokjaer, S.; Brange, J.; Vyas, S.; Uversky, V. N.; Fink, A. L. Effect of environmental factors on the kinetics of insulin fibril formation: Elucidation of the molecular mechanism. *Biochemistry.* **2001**, *40*, 6036-6046.
(38) Arosio, P.; Knowles, T. P. J.; Linse, S. On the lag phase in amyloid fibril formation. *PCCP.* **2015**, *17*, 7606-7618.
(39) Shoffner, S. K.; Schnell, S. Estimation of the lag time in a subsequent monomer addition model for fibril elongation. *PCCP.* **2016**, *18*, 21259-21268.
(40) Temkin, M. I. Relaxation rate of a 2-stage catalytic reaction. *Kinet. Catal.* **1976**, *17*, 1095 - 1099.
(41) Shapatina, E. N.; Kuchaev, V. L.; Temkin, M. I. Relaxation of rate of ammonia synthesis. *Kinet. Catal.* **1985**, *26*, 575-582.
(42) Kobayashi, M. Characterization of transient response curves in heterogeneous catalysis—I Classification of the curves. *Chem. Eng. Sci.* **1982**, *37*, 393-401.
(43) Kobayashi, M. Characterization of transient response curves in heterogeneous catalysis - 2. Estimation of the reaction mechanism in the oxidation of ethylene over a silver catalyst from the mode of the transient response curves. *Chem. Eng. Sci.* **1982**, *37*, 403-409.
(44) Kobayashi, M.; Maeda, Y.; Takahashi, N. Discrimination of rival kinetic models in heterogeneous catalysis by the dynamic behaviour of products. *Journal of Chemical Technology and Biotechnology, Chemical Technology.* **1983**, *33 A*, 219-226.
(45) Omojola, T.; Cherkasov, N.; McNab, A. I.; Lukyanov, D. B.; Anderson, J. A.; Rebrov, E. V.; van Veen, A. C. Mechanistic Insights into the Desorption of Methanol and Dimethyl Ether Over ZSM-5 Catalysts. *Catal. Lett.* **2018**, *148*, 474-488.
(46) Wei, Z.; Chen, Y. Y.; Li, J.; Guo, W.; Wang, S.; Dong, M.; Qin, Z.; Wang, J.; Jiao, H.; Fan, W. Stability and Reactivity of Intermediates of Methanol Related Reactions and C-C Bond Formation over H-ZSM-5 Acidic Catalyst: A Computational Analysis. *Journal of Physical Chemistry C.* **2016**, *120*, 6075-6087.
(47) Omojola, T.; Cherkasov, N.; Rebrov, E. V.; Lukyanov, D. B.; Perera, S. P. Zeolite minilith: A unique structured catalyst for the methanol to gasoline process. *Chemical Engineering and Processing - Process Intensification.* **2018**, *131*, 137-143.
(48) Omojola, T.; Lukyanov, D. B.; van Veen, A. C. Transient kinetic studies and microkinetic modeling of primary olefin formation from dimethyl ether over ZSM-5 catalysts. *Int. J. Chem. Kinet.* **2019**, *51*, 528-537.
(49) Chowdhury, A. D.; Paioni, A. L.; Houben, K.; Whiting, G. T.; Baldus, M.; Weckhuysen, B. M. Bridging the Gap between the Direct and Hydrocarbon Pool

Mechanisms of the Methanol-to-Hydrocarbons Process. *Angewandte Chemie - International Edition.* **2018**.

(50) Giannetto, G.; Monque, R.; Galiasso, R. Transformation of LPG into Aromatic Hydrocarbons and Hydrogen over Zeolite Catalysts. *Catalysis Reviews.* **1994**, *36*, 271-304.

(51) Naccache, C. Dehydrocyclization of Alkanes Over Zeolite-Supported Metal Catalysts: Monofunctional or Bifunctional Route AU - MÉRIAUDEAU, PAUL. *Catalysis Reviews.* **1997**, *39*, 5-48.

(52) Joshi, Y. V.; Bhan, A.; Thomson, K. T. DFT-Based Reaction Pathway Analysis of Hexadiene Cyclization via Carbenium Ion Intermediates: Mechanistic Study of Light Alkane Aromatization Catalysis. *The Journal of Physical Chemistry B.* **2004**, *108*, 971-980.

(53) Olsbye, U.; Svelle, S.; Lillerud, K. P.; Wei, Z. H.; Chen, Y. Y.; Li, J. F.; Wang, J. G.; Fan, W. B. The formation and degradation of active species during methanol conversion over protonated zeotype catalysts. *Chem. Soc. Rev.* **2015**, *44*, 7155-7176.

(54) Gleaves, J. T.; Ebner, J. R.; Kuechler, T. C. Temporal Analysis of Products (TAP) — A Unique Catalyst Evaluation System with Submillisecond Time Resolution. *Catalysis Reviews.* **1988**, *30*, 49-116.

(55) Levenspiel, O.: *Chemical Reaction Engineering*; 3rd ed.; John Wiley & Sons 1999.

(56) Rouquerol, J.; Llewellyn, P.; Rouquerol, F.: Is the BET equation application to microporous adsorbents? In *Stud. Surf. Sci. Catal.*; Llewellyn, P., Rodriquez-Reinoso, F., Rouquerol, J., Seaton, N., Eds.; Elsevier, 2007; Vol. 160; pp 49-56.

(57) Hinrischen, O.; van Veen, A. C.; Zanthoff, H. W.; Muhler, M.: TAP Reactor Studies. In *In-Situ Spectroscopy in Heterogeneous Catalysis*; Haw, J. F., Ed.; Wiley-VCH: WeinHeim, 2002.

(58) Dewaele, O.; Geers, V. L.; Froment, G. F.; Marin, G. B. The conversion of methanol to olefins: A transient kinetic study. *Chem. Eng. Sci.* **1999**, *54*, 4385-4395.

(59) Pérez-Uriarte, P.; Ateka, A.; Gamero, M.; Aguayo, A. T.; Bilbao, J. Effect of the Operating Conditions in the Transformation of DME to olefins over a HZSM-5 Zeolite Catalyst. *Ind. Eng. Chem. Res.* **2016**, *55*, 6569-6578.

(60) Weisz, P. B.; Frilette, V. J.; Maatman, R. W.; Mower, E. B. Catalysis by crystalline aluminosilicates II. Molecular-shape selective reactions. *J. Catal.* **1962**, *1*, 307-312.

(61) Avrami, M. Kinetics of Phase Change. I General Theory. *The Journal of Chemical Physics.* **1939**, *7*, 1103-1112.

(62) Avrami, M. Kinetics of Phase Change. II Transformation-Time Relations for Random Distribution of Nuclei. *The Journal of Chemical Physics.* **1940**, *8*, 212-224.

(63) Avrami, M. Granulation, Phase Change, and Microstructure Kinetics of Phase Change. III. *The Journal of Chemical Physics.* **1941**, *9*, 177-184.

(64) Richards, F. J. A Flexible Growth Function for Empirical Use. *J. Exp. Bot.* **1959**, *10*, 290-301.

(65) Verhulst, P. F. Recherches mathématiques sur la loi d'accroissement de la population. *Nouveaux mémoires de l'Académie Royale des Sciences et Belles-Lettres de Bruxelles.* **1845**, *18*, 14-54.

(66) Morgan, K.; Maguire, N.; Fushimi, R.; Gleaves, J. T.; Goguet, A.; Harold, M. P.; Kondratenko, E. V.; Menon, U.; Schuurman, Y.; Yablonsky, G. S. Forty years of temporal analysis of products. *Catalysis Science and Technology.* **2017**, *7*.

(67) Kanervo, J. M.; Kouva, S.; Kanervo, K. J.; Kolvenbach, R.; Jentys, A.; Lercher, J. A. Prerequisites for kinetic modeling of TPD data of porous catalysts-Exemplified by toluene/H-ZSM-5 system. *Chem. Eng. Sci.* **2015**, *137*, 807-815.

(68) Redhead, P. A. Thermal desorption of gases. *Vacuum.* **1962**, *12*, 203-211.

(69) Chansai, S.; Burch, R.; Hardacre, C. The use of Short Time on Stream (STOS) transient kinetics to investigate the role of hydrogen in enhancing NOx reduction over silver catalysts. *J. Catal.* **2012**, *295*, 223-231.

(70) Demmin, R. A.; Gorte, R. J. Design parameters for temperature-programmed desorption from a packed bed. *J. Catal.* **1984**, *90*, 32-39.
(71) Hinz, A.; Andersson, A. Propane ammoxidation on an Al-Sb-V-W-oxide catalyst. A mechanistic study using the TAP-2 reactor system. *Chem. Eng. Sci.* **1999**, *54*, 4407-4421.
(72) Park, T. Y.; Froment, G. F. Kinetic modeling of the methanol to olefins process. 1. Model formulation. *Ind. Eng. Chem. Res.* **2001**, *40*, 4172-4186.
(73) Wang, W.; Hunger, M. Reactivity of surface alkoxy species on acidic zeolite catalysts. *Acc. Chem. Res.* **2008**, *41*, 895-904.
(74) Wang, C.; Chu, Y.; Xu, J.; Wang, Q.; Qi, G.; Gao, P.; Zhou, X.; Deng, F. Extra-Framework Aluminum-Assisted Initial C−C Bond Formation in Methanol-to-Olefins Conversion on Zeolite H-ZSM-5. *Angew. Chem. Int. Ed.* **2018**, *57*, 10197-10201.
(75) Li, S.; Zheng, A.; Su, Y.; Zhang, H.; Chen, L.; Yang, J.; Ye, C.; Deng, F. Brønsted/lewis acid synergy in dealuminated HY zeolite: A combined solid-state NMR and theoretical calculation study. *J. Am. Chem. Soc.* **2007**, *129*, 11161-11171.
(76) Li, J.; Wei, Z.; Chen, Y.; Jing, B.; He, Y.; Dong, M.; Jiao, H.; Li, X.; Qin, Z.; Wang, J.; Fan, W. A route to form initial hydrocarbon pool species in methanol conversion to olefins over zeolites. *J. Catal.* **2014**, *317*, 277-283.
(77) Chen, Z.; Ni, Y.; Zhi, Y.; Wen, F.; Zhou, Z.; Wei, Y.; Zhu, W.; Liu, Z. Coupling of Methanol and Carbon Monoxide over H-ZSM-5 to Form Aromatics. *Angew. Chem. Int. Ed.* **2018**, *57*, 12549-12553.